Chapter 9

Observed binaries with compact objects

This chapter provides an overview of observed types of binaries in which one or both stars are compact objects (white dwarfs, neutron stars or black holes). In many of these systems an important energy source is accretion onto the compact object.

9.1 Accretion power

When mass falls on an object of mass M and with radius R, at a rate $\dot{M}$, a luminosity $L_{\rm acc}$ may be produced:

$$L_{\rm acc} = \frac{GM\dot{M}}{R} \tag{9.1}$$

The smaller the radius, the more energy can be released. For a white dwarf with $M \approx 0.7\,M_\odot$ and $R \approx 0.01\,R_\odot$, this yields $L_{\rm acc} \approx 1.5 \times 10^{-4}\dot{M}c^2$. For a neutron star with $M \approx 1.4\,M_\odot$ and $R \approx 10\,$km, we find $L_{\rm acc} \approx 0.2\dot{M}c^2$ and for a black hole with Scwarzschild radius $R \sim 2GM/c^2$ we find $L_{\rm acc} \sim 0.5\dot{M}c^2$, i.e. in the ideal case a sizable fraction of the rest mass may be released as energy. This accretion process is thus potentially much more efficient than nuclear fusion.

However, the accretion luminosity should not be able to exceed the Eddington luminosity,

$$L_{\rm acc} \leq L_{\rm Edd} = \frac{4\pi cGM}{\kappa} \tag{9.2}$$

where κ is the opacity, which may be taken as the electron scattering opacity, $\kappa_{\rm es} = 0.2(1 + X)\,{\rm cm}^2/{\rm g}$ for a hydrogen mass fraction X. Thus the compact accreting star may not be able to accrete more than a fraction of the mass that is transferred onto it by its companion. By equating $L_{\rm acc}$ to $L_{\rm Edd}$ we obtain the maximum accretion rate,

$$\dot{M}_{\rm Edd} = \frac{4\pi cR}{\kappa} \tag{9.3}$$

The remainder of the mass may be lost from the binary system, in the form of a wind or jets blown from the vicinity of the compact star, or it may accumulate in the accretor's Roche lobe or in a common envelope around the system. For a white dwarf with $R \approx 0.01\,R_\odot$ accreting hydrogen-rich gas ($X = 0.7$) we find $\dot{M}_{\rm Edd} \approx 1.2 \times 10^{-5}\,M_\odot/{\rm yr}$, and for a neutron star with $R \approx 10\,$km, $\dot{M}_{\rm Edd} \approx 1.7 \times 10^{-8}\,M_\odot/{\rm yr}$.

9.2 White dwarf binaries

Among main-sequence binaries with unseen companions, a sizable fraction will contain a white dwarf that has cooled beyond detection. Here we discuss only those systems in which the white dwarf is

Table 9.1. Some close white-dwarf binaries. Masses and radii are given in solar units. If no eccentricity is given the orbit is circular. Mass values in *italics* indicate the measured mass function, rather than the mass.

name	spectra	P (d)	e	M_1	M_2	R_1	R_2
close binaries inside planetary nebulae							
KV Vel	sdO + CIIIe	0.357		0.63	0.23	0.16	0.40
UU Sge	sdO + M?	0.465		0.63	0.29	0.33	0.54
V477 Lyr	sdO + M?	0.472		0.51	0.15	0.17	0.46
BE UMa	sdO + M?	2.29		0.7:	0.36:	0.08:	0.7:
V651 Mon	sdO + A5Vm:	16.0	0.07:		*0.0073*		
detached white dwarf-main sequence binaries							
HR Cam	WD + M	0.103		0.41	0.10	0.018	0.125
13471-128	WD + M3.5/4	0.151		0.78	0.43	0.011	0.42
NN Ser	WD + M5-6	0.130		0.57	0.12	0.019	0.17
CC Cet	WDA2 + M4.5e	0.284		0.39	0.18		0.21
GK Vir	WDAO + M3-5V	0.344		0.51	0.10		0.15
V471 Tau	WD + K2V	0.521		0.84	0.93	0.011	0.96
Feige 24	WD + M1.5V	4.23		0.47	0.30	0.032	
double white dwarf binaries							
0957-666	WDA + WDA	0.061		0.32	0.37		
1101+364	WDA3 + WDA	0.145		0.33	0.29		
1704+481a	WDA4 + WD	0.145		0.56	0.39		
HE 1414-0848	WD + WD	0.518		0.55	0.71		
1399+144	WD + WD	2.209		0.44	0.44		

observed directly, or its presence is revealed by current or past interaction with its companion. Binaries consisting of a white dwarf plus a normal star can be divided into systems with close orbits ($P \lesssim 10$ d) and those with relatively wide orbits ($P \gtrsim 100$ d).

9.2.1 Close detached white-dwarf binaries

Several white dwarfs have been detected in a close detached orbit ($P \lesssim 10$ d) around a low-mass main-sequence star. Some examples are given in Table 9.1. In these systems the orbits are much smaller than the size of the red-giant progenitor of the white dwarf, and their formation requires strong mass and angular momentum loss in the form of a common envelope phase and spiral-in (to be discussed in § 10.2).

Closely related are so-called double cores of planetary nebulae, in which the hot nucleus of the nebula which will later cool into a white dwarf is accompanied by a low-mass star in a close orbit. About 5 to 10 per cent of all planetary nebulae have such double cores. In these systems the nebula is probably the ejected common envelope that formed the close binary. These detached binaries may evolve, by means of either angular momentum loss from the orbit (to be discussed in § 11.3) or nuclear expansion of the main-sequence star, into one of the two types of semi-detached, interacting binaries discussed in § 9.2.2.

Double white dwarfs Many short period binaries consisting of two white dwarfs have been discovered in recent years, see Table 9.1 for a few examples. Their orbital periods range from $P \sim 0.06$–30 d. In most cases the masses of the white dwarfs are low, $\lesssim 0.45\,M_\odot$, which means that they must be composed of helium rather than carbon and oxygen. The masses of the two white dwarfs are often rather similar,

Table 9.2. Some cataclysmic variables and supersoft X-ray sources. Masses and radii are given in solar units. Types: CN - classical nova; DN - dwarf nova; MP - magnetic polar; IP - intermediate polar; UCB - ultra-compact binary; SSX - supersoft X-ray source.

name	spectra	type	P (d)	M_1	M_2	R_1	R_2
AM CVn	He em	UCB	0.012		0.04:		
OY Car	sdBe + M7-8	DN	0.063	0.685	0.07		0.127
Z Cha	sdBe + M5.5V	DN	0.075	0.84	0.125		0.17
AM Her	sdBe + M4V	MP	0.129	0.44	0.29		0.33
U Gem	sdBe + M4V	DN	0.177	1.26	0.57		0.51
DQ Her	sdBe + M3V	CN, IP	0.194	0.60	0.40		0.49
BT Mon	sdBe + G8V	CN	0.334	1.04	0.87		0.89
GK Per	sdBe + K1IV	CN, DN	2.00	0.9:	0.5:		2.5:
V Sge	WN: + B8:	SSX	0.514	0.9:	3.3:		2.1
U Sco	sdBe + F8V	SSX	1.23	1.55:	0.88		2.1

which provides important clues for their formation. The closest systems among them are expected to merge within a Hubble time due to angular momentum loss by gravitational radiation.

9.2.2 Cataclysmic variables and related systems

Cataclysmic variables The name of this group derives from their outbursting nature, they comprise the *classical novae* and related systems, see Table 9.2. They consist of a low-mass main-sequence star and a white dwarf, the MS star is filling its Roche lobe and transferring mass to the WD via an accretion disk. Orbital periods are typically $0.05\,\mathrm{d} \lesssim P \lesssim 0.5\,\mathrm{d}$, with a few exceptions. Inbetween outbursts, the accretion disk is often the main source of light in the system. The white dwarf is more massive than its companion, $q = M_{\rm MS}/M_{\rm WD} \lesssim 0.7$ so that Roche-lobe overflow is stable and occurs at a low rate ($\dot{M} \sim 10^{-11}$–$10^{-9}\,M_\odot$/yr). The low accretion rate leads to hydrogen piling up on the surface of the white dwarf, until it ignites in a flash when the pressure and temperature at the bottom of the accreted layer are high enough for fusion. The resulting thermonuclear runaway leads to the observed nova outbursts during which the visual luminosity increases by a factor 10^4–10^6.

Probably all cataclysmic variables undergo nova outbursts, but only in a subset of them have they been observed. This is consistent with the expected time between thermonuclear flashes, $\gtrsim 10^4$ years. Many other CVs, known as *dwarf novae*, show outbursts of a different kind, milder in nature (up to a factor 10^2 in luminosity) and occurring every few weeks. These are probaly the result of an instability in the accretion disk, which builds up until the viscosity suddenly increases and the accumulated mass is rapidly dumped onto the white dwarf. In other systems, known as *polars*, the white dwarf is highly magnetized and dominates the accretion flow, either completely (magnetic polars, in which the accretion disk is absent and the white dwarf rotation is locked with the orbit) or partly (intermediate polars, which have small accretion disks truncated on the inside by the white-dwarf magnetosphere).

Supersoft X-ray sources The sensitivity of ROSAT to photons with energies $\lesssim 500\,\mathrm{eV}$ has led to the discovery of a new class of X-ray sources that emits only at these low energies. Various types of objects could give rise to such very soft X-ray emission. The most luminous persistent sources, with $L \sim 10^{36-38}$ erg/s and blackbody temperatures of several times 10^5 K, are white dwarfs undergoing steady nuclear burning of hydrogen on their surfaces. Theoretical accretion models show that this happens if a WD accretes at a steady rate of $1\text{–}2 \times 10^{-7}\,M_\odot$/yr. This is typically what is expected for thermal-

Table 9.3. Some symbiotic and barium-star binaries. The last column gives the mass function of the giant (secondary) component; radial velocity variations of the white dwarf are generally not measured.

name	spectra	P (d)	e	$f(M_2)$
	symbiotic binaries			
T CrB	Be + M4III	227.7	0	0.32
AG Dra	sdOe + K3pII	549	0.13	0.008
BD Cam	WD + M3/S5	597	0.09	0.037
	barium star systems			
HD 77247	? + G7IIBa	80.53	0.09	0.0050
105 Her	? + K3IIBa	486	0.36	0.135
ξ^1 Cyg	WD + G7IIIBa	1642	0	0.035
ζ Cap	WD + G5IbBa	2380	0.28	0.0042
ζ Cyg	WD + G8IIIBa	6489	0.22	0.0227

timescale mass transfer from a main-sequence or subgiant donor of 1.3–2.5 $M_\odot$ to a less massive white dwarf. Their orbital periods typically range from 0.2 to 4 d, making SSXs the higher-mass analogues of CVs. The steady accretion rate may bring the white dwarf over the Chandrasekhar limit, and these systems are currently considered as the most likely progenitors of Type Ia supernovae. (In contrast, in CVs the nova outbursts eject most or all of the previously accreted mass so that the white dwarf mass does not grow.)

9.2.3 Symbiotic binaries and related systems

Symbiotic stars show the combined spectrum of a cool giant superimposed with emission lines of hydrogen and helium. The emission spectrum comes from a hot white dwarf that accretes matter from its red giant or AGB companion, either from the strong stellar wind of the giant or in some cases by Roche-lobe overflow. The accretion (at rates up to 10^{-7} $M_\odot$/yr) heats the white dwarf so that it competes in luminosity with the red giant (100–1000 $L_\odot$) and becomes visible. The orbital periods of symbiotic binaries range from $P \sim 10^2$–10^4 days. Several symbiotics show nova outbursts, often recurrent in nature (symbiotic novae) and some are also observed as supersoft X-ray sources. Hence the classes of symbiotic binaries and cataclysmic variables partly overlap.

Related to symbiotic binaries in their evolutionary history, but different in appearance, are the barium and CH stars. They are red giants or subgiants in binaries with similar periods ($P \sim 10^2$–10^4 d) but the white dwarf is usually not directly observed. The presence of a white dwarf is inferred, apart from the radial velocity variations, from the abundance anomalies in the spectrum of the (sub)giant which is enhanced in carbon and heavy s-process elements, in particular barium. These elements were produced by the progenitor of the white dwarf while it was an AGB star and have been transferred to the lower-mass main-sequence companion, now seen as a giant.

9.3 Neutron star and black hole binaries

Binaries containing a neutron star or a black hole can be observed as strong sources of X-rays as a result of accretion onto the compact object (eq. 9.1) in which case they are known as X-ray binaries. In the absence of accretion, a neutron star (but not a black hole) in a binary can be observed as a binary radio pulsar (§ 9.3.4).

Investigation of the properties of the brightest X-ray sources showed that they can be divided in two clearly separate types (Figure 9.2). Some sources emit their X-rays partially pulsed, others only show irregular variations. Many systems in the latter category occasionally show sudden surges in the X-ray flux: the X-ray bursts.

9.3.1 X-ray pulsars: high-mass X-ray binaries

The model for X-ray pulsars is that they are neutron stars with a strong dipolar magnetic field, which focusses the accreting matter to the magnetic poles, where it is stopped and emits X-rays. As the poles rotate in and out of view, we observe pulses of X-rays. The spectra of X-ray pulsars are hard, and photons are detected to energies above 50 keV. Signs of the magnetic fields are thought to have been detected in the form of cyclotron absorption lines in the X-ray spectra.

Optical identification was not easy in the early days, as the X-ray pulsars are located in the Galactic Plane, which means that the relatively large positional error boxes are crowded with stars. Nonetheless, many X-ray pulsars were succesfully identified, and their optical counterparts almost invariably are massive O or B stars. The X-ray pulse period varies due to the orbital motion of the neutron star around its companion; when the radial velocity curve of the O or B star can be measured as well, we have a double-lined spectroscopic binary. If in addition the neutron star is eclipsed by its companion, classical binary techniques can be employed to determine the masses of both stars. The neutron star masses cluster around 1.4 $M_\odot$, as expected from theory.

Some X-ray sources with an O or B companion star do not show pulses. The X-ray source in these may still be a neutron star. In some cases, however, which include Cyg X-1 and LMC X-3, the orbital velocity of the O or B supergiant indicates a mass for the compact star in excess of the maximum mass that is possible for a neutron star, and it is concluded that the compact star must be a black hole. The X-ray spectra of these black hole candidates contain more photons both at low energies (< 1 keV) and at high energies (up to > 100 keV) than the pulsar spectra.

Mass determinations are feasible in the systems with relatively short orbital periods, $P_{\rm orb} \lesssim 10$ d, in which the companion of the neutron star is an O or B supergiant. Many systems have rather longer orbital periods, up to more than a year. In these, the companion is usually a Be star, i.e. a rapidly rotating B star, and the X-ray emission is only detected occasionally. Taking selection effects against detection of

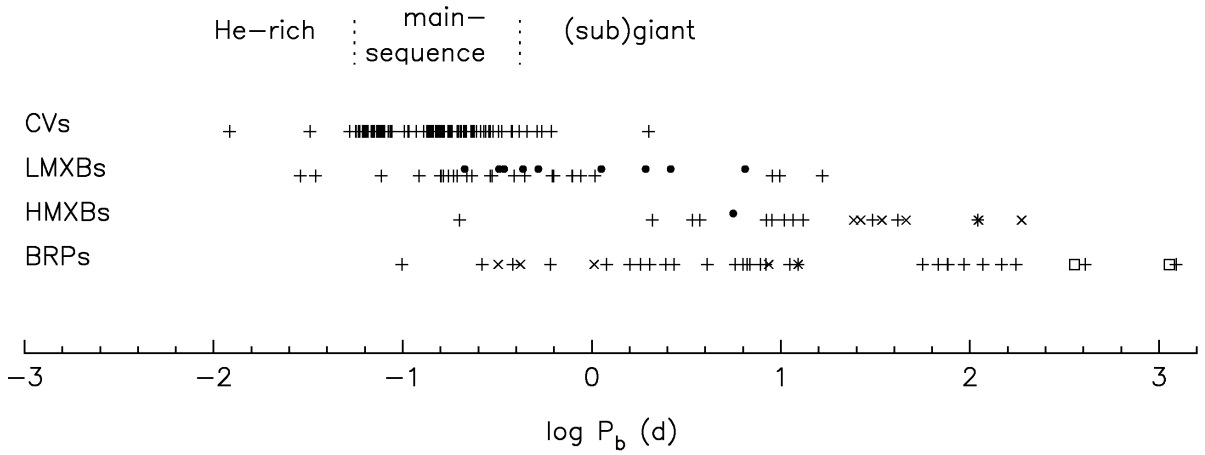

Figure 9.1. Orbital periods of cataclysmic variables, X-ray binaries and binary radio pulsars in our Galaxy. Each symbol indicates one system. For the X-ray binaries • indicates a system with a black hole, and × a Be donor star. For the binary radio pulsars + indicates a system with a low-mass white dwarf companion, × a system with a high-mass white dwarf or neutron star companion, and □ a main-sequence companion.

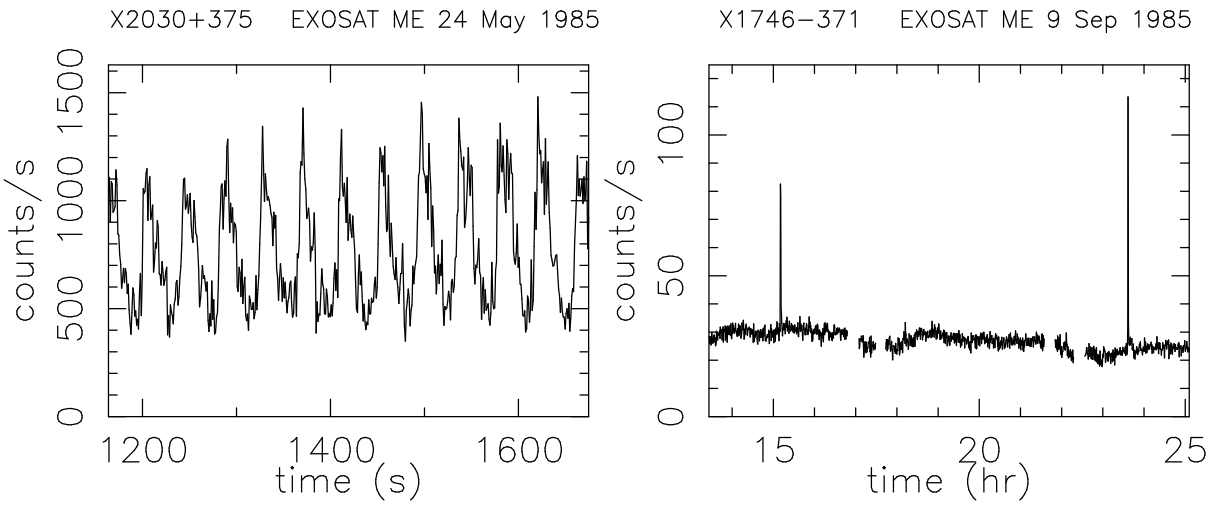

Figure 9.2. X-ray lightcurves, obtained with EXOSAT, of an X-ray pulsar, EXO 2030+375 (left), and of a burster, X1746-371, with two bursts visible (right).

such transient hard X-ray sources into account, we conclude that the Be-star + X-ray-pulsar binaries are in fact much more common (a few thousand in the Galaxy) than the supergiant + X-ray-pulsar systems (a dozen in the Galaxy). For both types of systems we find that the X-ray luminosity emitted near the neutron star is of the order of the optical luminosity of the O or B star.

The pulse periods of all X-ray pulsars vary, on time scales ranging from $P/\dot{P} \approx 100\,\mathrm{yr}$ to $10^6\mathrm{yr}$. These short time scales indicate that the moment of inertia, and hence the radius, of these objects are very small, in agreement with the theoretical estimates for neutron-star radii of $\sim 10\,\mathrm{km}$.

9.3.2 X-ray bursters: low-mass X-ray binaries

Soon after the discovery of the X-ray bursts, it was realized that these are caused by the sudden fusion into carbon of a helium layer on a neutron star, deposited there by the accretion of hydrogen which fuses immediately into helium. Thus, a burst is the neutron-star analogue of a nova outburst for a white dwarf. The X-ray spectra of the X-ray bursts have characteristic temperatures of $kT \lesssim 5\,\mathrm{keV}$. The steady X-ray spectrum of the luminous burst sources is soft; less luminous sources have power-law spectra. The spectra of sources of variable luminosity change accordingly.

Orbital periods for X-ray sources without pulses could be determined in larger numbers only after the launch of EXOSAT, whose wide orbit allowed four days of uninterrupted observing, and after the introduction of CCD photometry, which is capable of detecting small flux variations accurately. The orbital periods span the same range as those of the cataclysmic variables, which by analogy is taken to suggest that the companion to the neutron star is a low-mass star, close to the main sequence. These X-ray sources are therefore called low-mass X-ray binaries. Direct measurements of the properties of the donor star are hard to obtain, because the optical luminosity is dominated by reprocessing into the optical of X-rays that impinge on the accretion disk around the neutron star. The optical luminosity of these systems is much less than the X-ray luminosity, $L_{\mathrm{opt}} \lesssim 0.01 L_{\mathrm{x}}$, say. Even though the low-mass X-ray binaries often are well away from the Galactic Plane, with $|z| \approx 1\,\mathrm{kpc}$, their low visual brightness impedes easy optical identification.

The thick accretion disk also is responsible for the paucity of eclipsing low-mass X-ray binaries: when the inclination is high enough for the neutron star to be eclipsed by its companion, the probability is high that it is hidden altogether by the accretion disk.

Some low-mass X-ray binaries are transient sources. In these, the optical flux from the disk disap-

Table 9.4. Name, position, pulse period, X-ray luminosity, orbital period and eccentricity, and (for high-mass systems) the spectral type of the donor, for representative X-ray binaries. Binaries containing a black hole, and transients are indicated with B and T, respectively. For transients, the luminosity is the luminosity at outburst maximum. It should be noted that luminosities are uncertain due to uncertain distances for many sources.

name	position	$P_{\rm pulse}$ (s)		log $L_{\rm X}$ (erg/s)	P (d)	e	sp.type
high-mass X-ray binaries							
LMC X-4	0532 – 66	13.5		38.6	1.4	0.011	O7III
LMC X-3	0538 – 64	-	B	38.5	1.7	∼0	BIII-IV
Cen X-3	1119 – 60	4.8		37.9	2.1	0.0007	O6.5II
SMC X-1	0115 – 74	0.7		38.8	3.9	<0.0008	B0I
Cyg X-1	1956 + 35	-	B	37.3	5.6	∼0	O9.7I
Vela X-1	0900 – 40	283		36.8	9.0	0.092	B0.5I
LMC tran	0535 – 67	0.069		T 39.0	16.7	∼0.7	B2IV
V635 Cas	0115 + 63	3.6		T 36.9	24.3	0.34	Be
BQ Cam	0331 + 53	4.4		T 35.8	34.3	0.31	Be
GX301-2	1223 – 62	696		37.0	41.5	0.47	B1-1.5
V725 Tau	0535 + 26	104		T 37.3	111.0	0.3-0.4	Be
low-mass X-ray binaries							
KZ TrA	1627 – 67	7.7		36.8	0.029		
V1405 Aql	1916 – 05			36.9	0.035		
UY Vol	0748 – 68			T 37.0	0.159		
V4134 Sgr	1755 – 34			36.8	0.186		
V616 Mon	0620 – 00		B	T 38.3	0.323		
N Mus 1991	1124 – 68		B	T 37.6	0.427		
Cen X-4	1455 – 31			T 38.0	0.629		
Sco X-1	1617 – 16			37.5	0.787		
V404 Cyg	2023 + 33		B	T 38.4	6.500		
peculiar systems							
Her X-1	1656 + 35	1.2		36.8	1.7	< 0.0003	A9-B
Cyg X-2	2142 + 38			38.0	9.843		A9
Cyg X-3	2030 + 41			38.0	0.2		WN
Cir X-1	1516 – 57			T 38.9	16.6		
SS433	1909 + 05			35.8	13.2		
bursting pulsar	1744 – 28	0.467		T 38.9	11.8		accretion bursts
bursting pulsar	1808 – 36	0.0025		T 36.8	0.084		thermonuclear bursts

pears with the X-ray flux, and the companion becomes optically detectable. The radial velocity curve of the companion can then be measured. The companions in transients indeed appear to be low-mass stars, i.e. with spectral type G or K. In an increasing number of such transients the mass function indicates that the compact accreting star is a black hole. The X-ray spectra of transients with a black hole are remarkably similar to those of transients with a neutron star; the difference being that at the brightest levels they have (relatively) more soft as well as more hard photons. The case of Cyg X-3 (see chapter 9.3.3) illustrates that the assumption of a low-mass donor remains insecure for most of the low-mass X-ray binaries.

Table 9.5. Position, pulse period, characteristic age ($\tau_c \equiv P/(2\dot{P})$, magnetic field strength, orbital period and eccentricity, and companion mass, for representative radio pulsar binaries. The companion masses marked $*$ were calculated for an assumed inclination of 60°.

position	$P_{\rm pulse}$ (ms)	$\log \tau_c$ (yr)	$\log B$ (G)	P (d)	e	M_c ($M_\odot$)
high-mass binary radio pulsars						
1534 + 12	37.9	8.4	10.0	0.42	0.2737	1.36
1913 + 16	59.0	8.0	10.4	0.32	0.6171	1.39
0655 + 64	195.6	9.7	10.1	1.03	<0.00005	>0.7
2303 + 46	1066.4	7.5	11.9	12.34	0.6584	1.5
low-mass binary radio pulsars						
1957 + 20	1.6	9.2	8.2	0.38	<0.001	0.02
1831 − 00	521.0	8.8	10.9	1.81	<0.005	0.07*
J0437 − 47	5.8	8.9	8.9	5.74	0.000018	0.17*
1855 + 09	5.4	9.7	8.5	12.33	0.000021	0.23
1953 + 29	6.1	9.5	8.6	117.35	0.00033	0.22*
0820 + 02	864.9	8.1	11.5	1232.40	0.0119	0.23*
antediluvian[a] radio pulsars						
1259 − 63	47.8			1236.8	0.870	Be
1820 − 11[b]	279.8	6.5	11.8	357.8	0.795	0.8*
single recycled radio pulsars						
1937 + 21	1.6	8.4	8.6			
1257 + 12[c]	6.2					

[a] i.e. in an evolutionary stage preceding mass transfer
[b] this pulsar is tentatively listed as antediluvian; alternatively, this system may be a high-mass binary radio pulsar
[c] this pulsar has three, possibly four planets.

9.3.3 Peculiar X-ray binaries

Pulsars with low-mass donors. Whereas most X-ray pulsars have O or B star companions, some have low- or intermediate-mass companions. The best known of these is Her X-1, which has a $\approx 2\,M_\odot$ companion, which is slightly evolved. Its age is therefore in excess of $\approx 5 \times 10^8$yr, and Her X-1 is an excellent example of an old neutron star with a strong magnetic field. The binary is also striking in being removed from the Galactic Plane, at $|z| \approx 3$ kpc. The X-ray pulsar 4U1626-67 has a companion in a ≈ 40 min orbit, whose mass must be less than $0.1\,M_\odot$. For some other pulsars, including 1E2259+59, there is no sign of any companion. It has been suggested that these are single, accreting from a disk; or that they do not accrete, but have very high magnetic fields.

Radio sources. The X-ray source 3A1909+05, with optical counterpart SS 433, is located in a shell of radio emission. The optical and X-ray spectra of this source show emission lines from a jet with velocity $v \approx 0.26c$, which precesses in about 165 days. The jet is detected directly in Very Long Baseline Interferometry radio observations. It is not clear whether the X-ray source is a neutron star or a black hole. Cyg X-3 has a 4.8 hr orbital period and was classified as a low-mass X-ray binary, until an infrared spectrum was obtained which shows the strong and broad Balmer emission lines characteristic of a Wolf Rayet star. Cyg X-3 has a double radio jet. Cir X-1 is another X-ray source with a radio jet, and is

remarkable for the sudden, extreme surges of the X-ray flux, possibly related to the periastron passage of the donor star.

The first *bursting pulsar* is a very bright transient which shows both pulses and bursts. The bursts are not thermonuclear, but probably due to variation in the accretion onto the neutron star. The second bursting pulsar is also a transient. Its bursts are genuine thermonuclear bursts. Its pulse period is very short, so that we may observe in this system a progenitor of a binary radio pulsar.

9.3.4 Binary radio pulsars

In the last decade, an increasing number of radio pulsars have been discovered in binaries. Two of these pulsars have a companion which is a massive O or B star. Most of the others have a companion believed to be a neutron star or a white dwarf. The pulsars in these other binaries are called recycled radio pulsars, and are generally characterized by short pulse periods, $P \gtrsim 1.5\,\mathrm{ms}$, and very low period derivatives, $P/\dot{P} \gtrsim 10^8\mathrm{yr}$, as compared to the pulse periods and period derivatives of ordinary radio pulsars, which have $P \sim 1\,\mathrm{s}$ and $P/\dot{P} \lesssim 10^7\mathrm{yr}$.

The pulse periods of binary radio pulsars vary with the orbital motion, which provides an indication of the mass of its companion. In three close binaries with two neutron stars, and one binary with a white dwarf and a neutron star, general relativistic effects allow accurate mass determinations. In some binaries, the companion to the recycled pulsar has a mass $M_c \gtrsim 1\,M_\odot$, and – with one exception – these orbits are eccentric. In the other binaries the mass of the companion is lower, $M_c \sim 0.2\,M_\odot$, and the orbits are (almost perfectly) circular (Fig. 9.3). As we will see, the first are thought to have evolved from high-mass X-ray binaries, the latter from low-mass X-ray binaries.

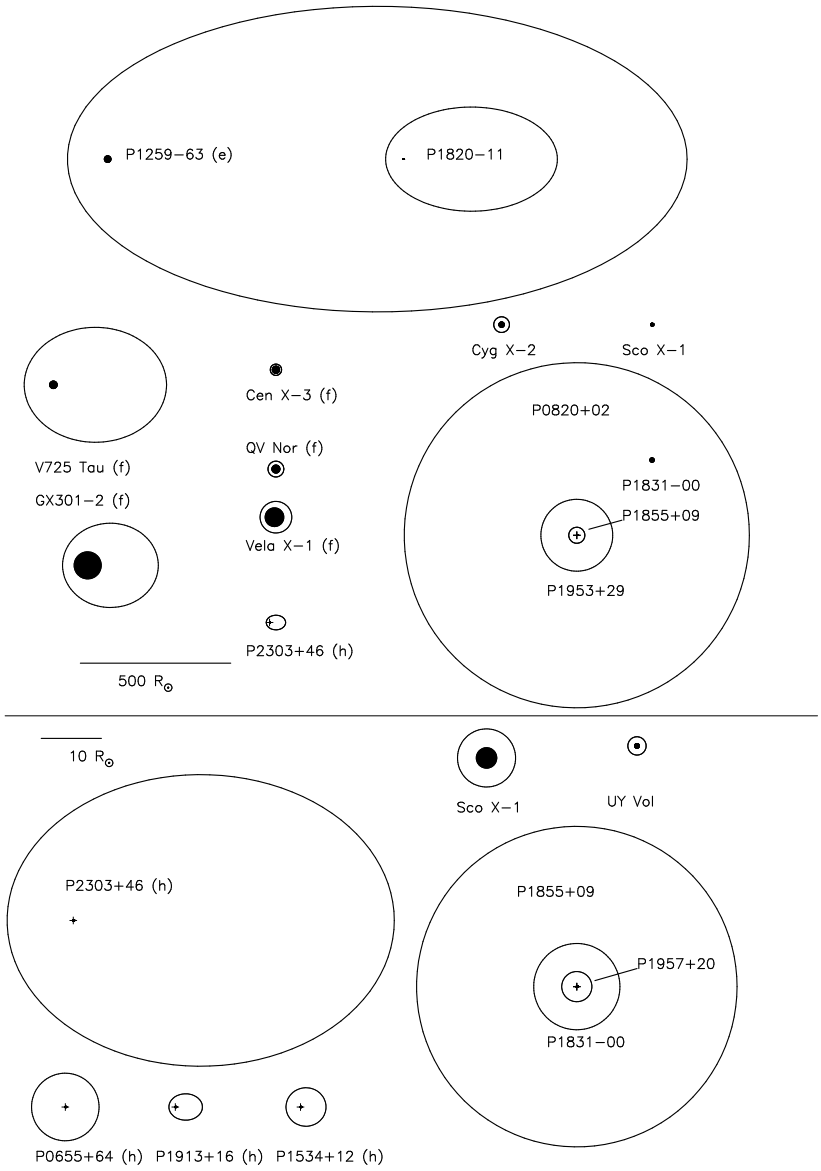

Figure 9.3. Drawing – to scale – of orbits of binaries with compact stars. An example of a massive binary in which one star has already exploded is PSR1259-63. Once the neutron star captures mass from its companion, it becomes an X-ray source like V725 Tau or GX301−2, which after spiral-in may form a binary with a recycled radio pulsar accompanied by a massive white dwarf (PSR0655+64) or after a second supernova by a second neutron star (PSR1913+16). PSR1820−11 may have a low-mass main-sequence companion, and evolve into a low-mass X-ray binary like Cyg X-2, which in turn may form a binary in which a recycled radio pulsar is accompanied by an undermassive white dwarf (PSR1855+09). (e,f,h): see Figure 11.1.

Chapter 10

Violent evolution processes

Two important processes can have a dramatic effect on a binary system, leading to drastic changes in its orbital parameters. In massive binaries, the supernova explosion of one of the stars causes sudden mass loss from the binary and probably also imparts a kick velocity to the remnant. The second process, common-envelope evolution and spiral-in, can affect binaries of all masses. Both these processes introduce major uncertainties in the evolution of binaries containing compact objects.

10.1 Mass loss in a supernova explosion

A neutron star or black hole can be formed from a massive star via a supernova explosion. The envelope of the exploding star is expelled. In a binary the loss of the envelope mass changes the binary parameters. To estimate this effect in a simple way, it is often assumed that the explosion occurs in a circular orbit, is instantaneous, and that the position and velocities of the stars are the same after the explosion as before the explosion. This implies that the distance a_i between the two stars before the explosion is the periastron distance after the explosion

$$a_i = (1 - e)a_f \tag{10.1}$$

and that the periastron velocity of the new orbit is the same as the orbital velocity in the pre-supernova orbit:

$$\frac{G(M_1 + M_2)}{a_i} = \frac{G(M_1 + M_2 - \Delta M)}{a_f}\frac{1 + e}{1 - e} \tag{10.2}$$

Substituting eq. (10.1) in eq. (10.2) gives the eccentricity of the post-supernova orbit:

$$e = \frac{\Delta M}{M_1 + M_2 - \Delta M} \tag{10.3}$$

We see that the binary is disrupted ($e > 1$) when more than half of the total mass is lost in the explosion, i.e. when $\Delta M > (M_1 + M_2)/2$.

Because of the mass loss, the velocity of the center of mass of the binary changes by v_s, given by

$$v_s = \frac{M_2 v_2 - (M_1 - \Delta M)v_1}{M_1 + M_2 - \Delta M} = ev_1 \tag{10.4}$$

where v_i is the orbital velocity of the star with mass M_i before the explosion. Massive binaries have small velocities; thus v_s is a good estimate for the system velocity of the binary after the supernova explosion.

If the orbit after the explosion is sufficiently small, it may be circularized by tidal interaction. From conservation of angular momentum, the radius a_c of the circular orbit can be written in terms of the semi-major axis of the eccentric orbit, or of the radius of the pre-supernova orbit

$$a_c = (1 - e^2)a_f = (1 + e)a_i \tag{10.5}$$

In reality, the correctness of the assumptions made to derive eqs. (10.1–10.5) is rather doubtful. Wide binaries are expected to have initially eccentric orbits. And from measurements of velocities of single radio pulsars, it appears that a single neutron star may receive an appreciable kick velocity at its birth, of several hundred km/s. It may be expected that a neutron star formed in a binary will also obtain a kick velocity at birth. This velocity can have an arbitrary direction and its effect on the orbit is therefore unpredictable. The presence of kick velocities introduces a major uncertainty in the evolution of a binary in which one star undergoes a supernova explosion.

10.1.1 Supernova explosion in an eccentric orbit

In an eccentric orbit, the relative velocity of the two stars when their distance to one another is r is given by

$$v^2 = G(M_1 + M_2)\left(\frac{2}{r} - \frac{1}{a}\right) \tag{10.6}$$

Denote the supernova progenitor mass with M_1, and the pre-explosion semi-major axis with a, and combine eq. (10.6) with a similar equation for the post-explosion orbit, with a compact star of mass $M_{1\rm n}$ and semi-major axis $a_{\rm n}$. Assuming that the instantaneous position r is not changed by the explosion, we then may write the ratio $a/a_{\rm n}$ as

$$\frac{a}{a_{\rm n}} = \frac{2a}{r} - \left(\frac{v_{\rm n}}{v}\right)^2 \frac{M_1 + M_2}{M_{1\rm n} + M_2}\left(\frac{2a}{r} - 1\right) \tag{10.7}$$

where $v_{\rm n}$ is the relative velocity between the two stars immediately after explosion.

The binary will be disrupted if the right hand side of eq. (10.7) is zero, which is the case for

$$\frac{r_{\rm d}}{2a} = 1 - \left(\frac{v}{v_{\rm n}}\right)^2 \frac{M_{1\rm n} + M_2}{M_1 + M_2} \tag{10.8}$$

$r_{\rm d}$ must be on the pre-explosion orbit, i.e. $1-e < r_{\rm d}/a < 1+e$, with e the eccentricity of the pre-explosion orbit. If the value for $r_{\rm d}/a$ found with eq. (10.8) is less than $1 - e$, e.g. when virtually no mass is lost, then the binary remains bound at all pre-explosion radii. If it is larger than $1 + e$, e.g. when virtually all mass is lost, then the binary is disrupted at all radii.

For intermediate values of $r_{\rm d}/a$, the binary will be disrupted at all $r < r_{\rm d}$, and thus the probability that this will happen is given by the fraction of the time that $r < r_{\rm d}$ in the binary orbit. We calculate this fraction by writing r in terms of the eccentric anomaly $\mathcal{E}$ (see Chapter 2)

$$r = a(1 - e\cos\mathcal{E}) \tag{10.9}$$

The eccentric anomaly may be related to the mean anomaly $\mathcal{M}$, which progresses linearly with time, via the equation of Kepler

$$\mathcal{M} = \mathcal{E} - e\sin\mathcal{E} \tag{10.10}$$

To calculate the probability that the supernova will dissolve the binary, we start by calculating $r_{\rm d}/a$ with eq. (10.8), and check whether $1 - e < r_{\rm d}/a < 1 + e$. If so, we continue by calculating the eccentric anomaly $\mathcal{E}_{\rm d}$ corresponding to $r_{\rm d}$ with eq. (10.9), and find the probability that the binary will be disrupted as the probability that the two stars are found at an r between periastron and $r_{\rm d}$ from eq. (10.10) as

$$\Pi_{\rm d} = \frac{\mathcal{E}_{\rm d} - e\sin\mathcal{E}_{\rm d}}{\pi} \tag{10.11}$$

In Fig. 10.1 the probability of survival, $\Pi_{\rm s} \equiv 1 - \Pi_{\rm d}$ is illustrated for a binary with initial semi-major axis of $100\,R_\odot$, in which a $10\,M_\odot$ star explodes to leave a $1.34\,M_\odot$ neutron star, and where the velocity

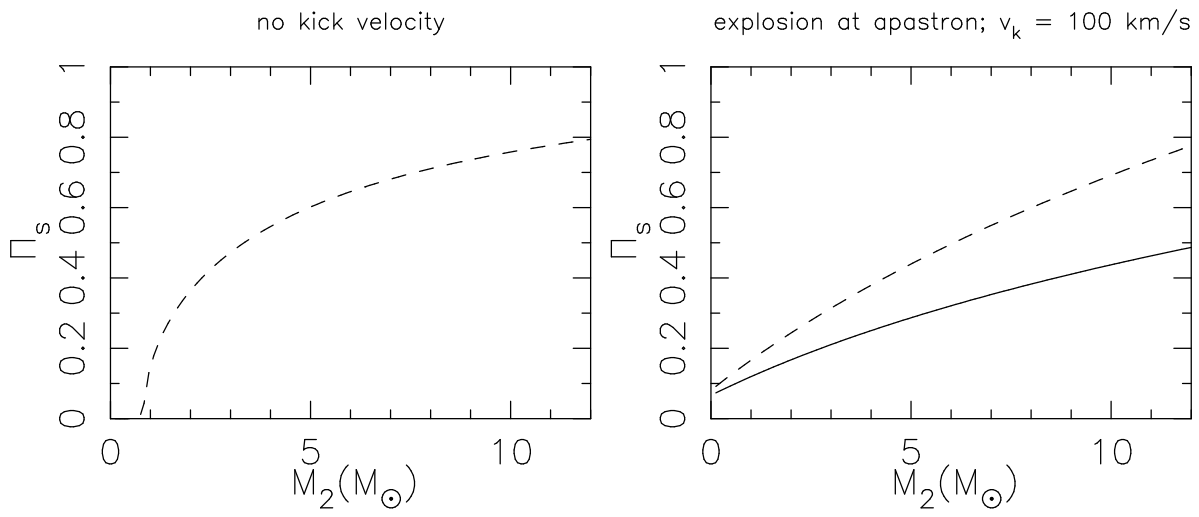

Figure 10.1. The probability Π_s, as a function of the mass M_2 of the non-exploding star, that the binary remains bound after a supernova explosion in which a $10\,M_\odot$ star leaves a $1.34\,M_\odot$ neutron star. (Left) without kick velocity in an eccentric orbit with $e = 0.6$. (Right) for the case in which the neutron star receives a kick velocity of $v_k = 100$ km/s in a circular orbit with $a = 100\,R_\odot$ (solid line) and in an orbit with $e = 0.6$ in which the explosion occurs at apastron (dashed line).

is unchanged: $v_n = v$, as a function of the companion mass M_2. For an initial circular orbit, eq. (10.9) shows that the binary is always disrupted for $M_2 < M_{2\rm crit} = 7.32\,M_\odot$, and always remains bound for $M_2 > M_{2\rm crit}$. For an initial orbit with eccentricity $e = 0.6$, we find that there is a finite probability that the binary survives down to very low companion masses, or that it is disrupted up to relatively high companion masses. The lowest possible companion mass for which the binary can remain bound is found by equating the pre-explosion velocity at apastron to the escape velocity after the explosion, at the same position:

$$v^2 = \frac{G(M_1 + M_2)(1-e)}{a(1+e)} = \frac{2G(M_{1n} + M_2)}{a(1+e)} \quad \Rightarrow \quad M_2 = \frac{(1-e)M_1 - 2M_{1n}}{1+e} \tag{10.12}$$

For the example shown in Fig. 10.1 this minimum mass is $M_2 = 0.825\,M_\odot$. Thus, in the absence of velocity kicks, even very low-mass stars have a finite probability of surviving the supernova explosion of their companion – after all, in an eccentric orbit more time is spent near apastron than near periastron.

10.1.2 Supernova with velocity kick

The calculations that we just discussed would lead to the conclusion that there could be many wide binaries in which a neutron star is accompanied by a low-mass companion, i.e. many radio pulsars would have an optical counterpart. As this appears not to be the case, we must conclude that most neutron stars acquire a kick velocity v_k at birth, which is added to the pre-explosion orbital velocity:

$$v_n^2 = v^2 + v_k^2 + 2vv_k\cos\theta \equiv (1 + f^2 + 2f\cos\theta)v^2 \tag{10.13}$$

where θ is the angle between the kick velocity and the orbital velocity before explosion, and where we have written the kick velocity in units of the pre-explosion velocity, $v_{\rm kick} \equiv fv$. This equation may be entered into eq. (10.8) to check whether the supernova explosion dissolves the binary in the presence of a kick.

To illustrate the effect of a kick we consider an explosion at apastron. The binary remains bound if the post-explosion velocity is less than the escape velocity:

$$(1 + f^2 + 2f\cos\theta)\frac{G(M_1 + M_2)(1-e)}{a(1+e)} \leq \frac{2G(M_{1\mathrm{n}} + M_2)}{a(1+e)} \quad \Rightarrow$$

$$\cos\theta \leq \cos\theta_{\mathrm{crit}} \equiv \frac{1}{2f}\left(\frac{2(M_{1\mathrm{n}} + M_2)}{(M_1 + M_2)(1-e)} - 1 - f^2\right) \tag{10.14}$$

The probability for this to happen is given by the probability that $\theta \geq \theta_{\mathrm{crit}}$, which for arbitrary direction of the kick is given by

$$\Pi_{\mathrm{s}} = \left(\int_{\theta_{\mathrm{crit}}}^{\pi} \sin\theta d\theta\right) / \left(\int_0^{\pi} \sin\theta d\theta\right) = \frac{1 + \cos\theta_{\mathrm{crit}}}{2} \tag{10.15}$$

and may be found directly from eq. (10.14), as illustrated in Fig. 10.1.

10.2 Common-envelope evolution

Two different circumstances can cause the companion of the mass-losing star to find itself engulfed by the envelope of the donor. The first of these is dynamically unstable mass mass transfer, which ensues when the donor cannot shrink fast enough to stay within its Roche lobe (Sect. 7.3). This usually occurs when the donor has a deep convective envelope (late case B and case C) and is of similar mass or more massive than its companion, or when the donor has a radiative envelope (early case B) but is much more massive than its companion, by a factor $\gtrsim 4$. The second circumstance arises when the spin angular momentum is more than $\frac{1}{3}$ times the orbital angular momentum, which causes tidal interaction to become unstable and the companion is literally dragged into the donor's envelope by tidal forces. This can occur when the mass ratio is very large.

Once the companion is inside the donor's envelope, the friction between the motion of the companion and the envelope removes angular momentum from the orbital motion, and releases energy. Thus, the orbit shrinks, and the envelope is brought into rotation and heated. This process continues until enough energy is added to the envelope to expel it. Alternatively, the companion star may spiral-in until it merges with the core of the mass donor.

This process, known as common-envelope evolution, was originally proposed in 1976 by B. Paczyński as an explanation for the existence of compact objects in very short-period binaries, such as cataclysmic variables, low-mass X-ray binaries and double white dwarfs (Chapter 9). The formation of such compact binaries requires the initial orbit to be wide enough for the progenitor of the compact object to expand to red giant dimensions and thus requires a substantial loss of orbital energy and angular momentum.

The outcome of a common envelope is often estimated based on the picture of conversion of orbital energy into binding energy of the envelope, which may or may not be thrown off eventually depending on how much orbital energy is available. We can measure the efficiency of the CE process as

$$\alpha_{\mathrm{CE}} = \frac{\Delta E_{\mathrm{bind}}}{\Delta E_{\mathrm{orb}}} \tag{10.16}$$

where

$$\Delta E_{\mathrm{orb}} = \frac{GM_{\mathrm{a}}M_{\mathrm{c,d}}}{2a_{\mathrm{f}}} - \frac{GM_{\mathrm{a}}M_{\mathrm{d}}}{2a_{\mathrm{i}}} \tag{10.17}$$

and $\Delta E_{\rm bind}$ is estimated as the binding energy of the envelope at the start of the CE process, i.e. as the binding energy of the donor envelope when it first fills its Roche lobe[1]:

$$\Delta E_{\rm bind} = \int_{M_{\rm c,d}}^{M_{\rm d}} \left(\frac{Gm}{r} - U \right) dm \tag{10.18}$$

$$\equiv \frac{GM_{\rm d}M_{\rm env,d}}{\lambda R_{\rm L,d}}. \tag{10.19}$$

The dimensionless parameter λ is a measure of the relative density distribution within the envelope, and of the contribution of internal energy (U) to the binding energy. We can then formally compute the ratio of final to initial separation as

$$\frac{a_{\rm f}}{a_{\rm i}} = \frac{M_{\rm c,d}}{M_{\rm d}} \frac{M_{\rm a}}{M_{\rm a} + 2M_{\rm env,d}/(\alpha_{\rm CE}\lambda r_{\rm L,d})} \tag{10.20}$$

where $r_{\rm L,d} = R_{\rm L,d}/a_{\rm i}$ is the relative Roche-lobe size of the the donor at the start of the CE, a function only of $M_{\rm d}/M_{\rm a}$. Usually the second term in the denominator of eq. (10.20) dominates over the first term, in which case we can simplify the equation to

$$\frac{a_{\rm f}}{a_{\rm i}} \approx \tfrac{1}{2}\alpha_{\rm CE}\lambda\, r_{\rm L,d}\, \frac{M_{\rm c,d}M_{\rm a}}{M_{\rm d}M_{\rm env,d}}. \tag{10.21}$$

The outcome of the common envelope phase is seen to depend on the product $\alpha_{\rm CE}\lambda$. The parameter λ can be calculated from a stellar structure model of the star at the moment it fills its Roche lobe. This can be done with reasonable accuracy, the main uncertainty being the exact boundary between the core and the envelope that will be ejected.

Two approaches have been taken to determine the efficiency parameter $\alpha_{\rm CE}$ of the common envelope process. Theoretically, $\alpha_{\rm CE}$ can be calculated from a three-dimensional hydrodynamic calculation of the spiral-in process. Much effort has one into such calculations, which are very challenging owing to the enormous range of spatial and temporal scales involved in the late phase of a common envelope. Realistic calculations must also include the effects of turbulence and radiative transfer, which is not yet feasible. The limited 3D hydrodynamical calculations done so far (which do not include the entire process from start to end) indicate values of $\alpha_{\rm CE} < 1$. These results should not be taken too literally yet. In particular the calculations do not take into account that, once the envelope has been spun up and the spiral-in has slowed down sufficiently, additional energy sources may aid in ejecting the envelope, such as nuclear power, accretion power or dynamical energy in envelope pulsations.

Another approach is to determine $\alpha_{\rm CE}$ observationally. Central binaries of planetary nebulae are very good objects for such a study, because the 'smoking gun' of the nebula shows that such binaries have only just emerged from a common envelope, i.e. they represent the conditions immediately following the spiral-in. The determination goes as follows. If the white dwarf is of low mass, $\lesssim 0.45\,M_\odot$, it must have formed as the helium core of a low-mass star on the red giant branch, which obeys a core-mass radius relation (Sect. 6.2.3). The mass of the white dwarf thus more or less fixes the size of the Roche lobe at the onset of the common envelope, such that the ratio $a_{\rm f}/a_{\rm i}$ can be determined from observed quantities. Applying eq. (10.20) to systems with a low-mass white dwarf and a main-sequence or other white-dwarf companion shows that $\alpha_{\rm CE}$ is in the range 0.2 to 1.

However, it has become clear that not all binaries for which dynamically unstable mass transfer is expected undergo spiral-in. Several symbiotic binaries and barium-star binaries have periods of a few hundred days, too short to have avoided unstable Roche-lobe overflow but too long to have experienced strong spiral-in. Furthermore, if one applies the technique described above in combination with eq. (10.20) to the first white dwarf formed in a double white-dwarf binary, one often finds *negative* values

[1]Note that others, e.g. Iben & Livio (1993), assume that the envelope has already expanded to a radius of $2a_{\rm i}$ when the CE phase starts.

of $\alpha_{\rm CE}$! The masses of the white dwarfs in such systems are often very similar, which means (applying the core-mass radius relation) that the separation did not change drastically between the formation of the first and the second white dwarf (Nelemans et al., 2000). This is inconsistent with either conservative mass transfer (which expands the orbit) or spiral-in. It appears that some binaries for which a common envelope is expected are capable of evolving very non-conservatively, but without strong orbital energy and angular momentum losses. How this process works is not understood. Additional energy sources are needed, such as nuclear energy, but this requires much longer timescales than the $\lesssim 10^3$ years normally associated with a common enevelope.

Exercises

10.1 The system V635 Cas (see Table 9.4) is an example of a Be X-ray binary. Assume a canonical mass of 1.35 $M_\odot$ for the neutron star and a mass of 15 $M_\odot$ for the Be star (typical of the Be components in such binaries).

(a) Why is it reasonable to assume a circular pre-supernova orbit in this system?

(b) Assuming the supernova was symmetric, compute the mass of the neutron-star progenitor just before the explosion.

10.2 Consider the example binary system discussed and plotted in Fig. 10.1. Assuming the pre-explosion orbit is circular with $a = 100\,R_\odot$, compute the maximum kick velocity for which a star of 1 $M_\odot$ can survive the supernova explosion of its 10 $M_\odot$ companion without the binary being disrupted.

10.3 Her X-1 is an X-ray binary with an orbital period of 1.7 days in which a main-sequence or subgiant star of 2.0 $M_\odot$ is transferring mass to its neutron star companion, which is observed as an X-ray pulsar. Fig. 10.2 shows two possible evolution scenarios.

The first one (the standard scenario) starts with a massive NS progenitor (10 $M_\odot$) and a 2 $M_\odot$ companion in a wide orbit (stage 1), which evolves via case C mass transfer (stage 2) and spiral-in into a close binary consisting of the helium core of the progenitor and the unchanged 2 $M_\odot$ companion with a short orbital period (stage 3). The helium core explodes and leaves a 1.4 $M_\odot$neutron star in an eccentric orbit (stage 4). Finally, after tidal interaction has circularized the orbit, Roche-lobe overflow starts and an X-ray binary with the observed parameters is formed (stage 5).

(a) Reconstruct this evolution scenario by filling in the missing values in the Figure, using the formulae encountered in the lectures. Also compute the eccentricity induced by the supernova at stage 4. Assume the SN explosion was symmetric (i.e. ignore the possible kick velocity) and assume that the spiral-in can be described by the energy balance prescription with $\alpha_{\rm CE} = \lambda = 1$. Also compute the system velocity of the binary after the explosion.

(b) The second scenario (accretion-induced collapse) involves an intermediate-mass progenitor, which initially forms a massive white dwarf (1.35 $M_\odot$) after case C mass transfer and spiral-in. When the companion fills its Roche lobe, it transfers mass to the white dwarf and pushes it over the Chandrasekhar limit when its mass is 1.44 $M_\odot$ (stage 4). A neutron star of 1.26$M_\odot$ is formed (stage 5). Compute the eccentricity and system velocity for this case, assuming no kick occurs.

Note: Her X-1 is at a distance of $z \approx 3$ kpc from the Galactic plane. If it was born in the plane, where the high-mass progenitors of neutron stars are, then the velocity as calculated in (b) is too low to carry it to its current position. Therefore accretion-induced collapse is not an option for Her X-1. To show this conclusively one must also investigate scenarios with kick velocities.

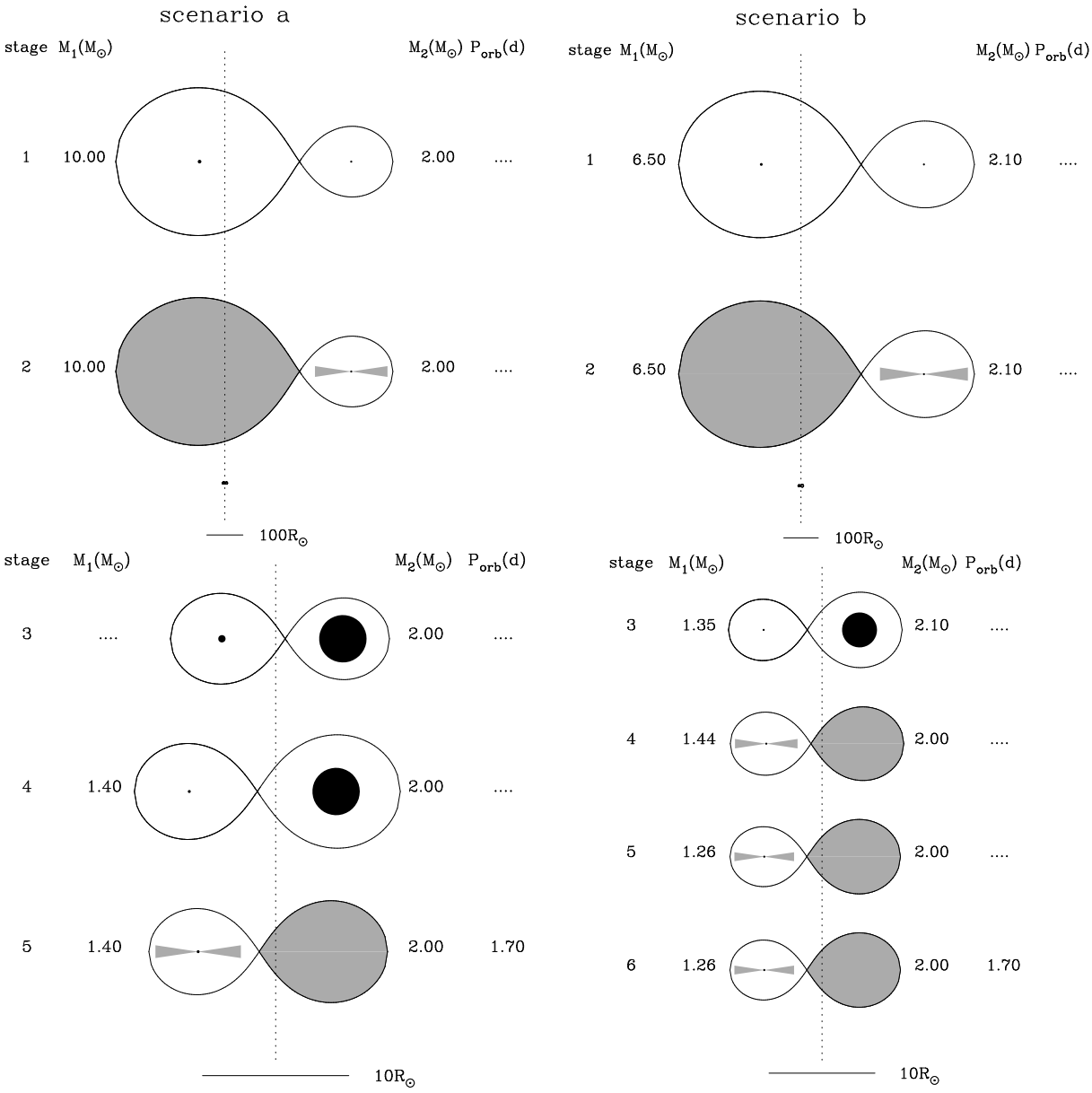

Figure 10.2. Drawing (to scale) of two scenarios for the evolution of Her X-1. Left: the standard scenario involving a massive primary; right: the accretion-induced collapse scenario. Note the change in scale after the spiral-in phase (stage 3).